Applied *Nanomaterials and smart Polymers,*
Online ISSN: 2981-0434
Vol. 1, No. 4

ANSP

In Situ Synthesis of Carbohydrate-Based Copper/Silver Hybrid Nanoparticles for the Preparation of Water-Repellent Fabric

Shabnam Karimnezhad mahbadi [1] , Mohsen Hosseinkhani [2,3,4]*

[1]Department of Textile Engineering, Yadegar-e-Imam Khomeini (RAH) Shahre Rey Branch, Islamic Azad University, Tehran, Iran.
[2]Nanotechnology Research Center, ST.C, Islamic Azad University, Tehran, Iran.
[3] Iranian Islamic Fashion and Clothing Research Center, Islamic Azad University, South Tehran Branch.
[4] Faculty of Fashion and Clothing, ST.C, Islamic Azad University, Tehran, Iran.

*** Corresponding Author:** Mh.hoseinkhani@iau.ac.ir

Abstract

Copper and silver metal nanoparticles and their compounds are of great significance across all industries due to their numerous properties and wide-ranging applications. Consequently, their synthesis has garnered considerable attention. Among the existing methods for nanoparticle synthesis, the reduction of metal salts in the presence of a stabilizer leads to the production of nanoparticles with controlled sizes. The use of green synthesis methods has attracted interest, as these approaches are environmentally friendly and employ natural, non-toxic materials.

In this study, the simultaneous hybrid synthesis of silver/copper nanoparticles was carried out via the reduction of metal salts using a green method. In addition to nanoparticle synthesis, the water-repellent properties of the treated samples were investigated. A natural reducing agent, maltose, along with silver and copper salts at various concentrations, was utilized. To control nanoparticle size, ascorbic acid was employed as a reducing and stabilizing agent at a constant concentration on cotton samples. For further characterization of the samples, tests including reflectance spectroscopy, wicking test, elemental analysis (EDX), scanning electron microscopy (SEM), X-ray diffraction (XRD), tensile strength, abrasion resistance, and bending stiffness were performed. The results obtained from these tests indicated significant differences among the samples. It was determined that among the specimens, the $A_1/C_1.M_1$ sample exhibited superior water repellency and resistance, which is attributed to the synthesized particle size (77.14 nm) in this particular sample.

Keywords: green synthesis, hybrid nanoparticles, silver/copper, water-repellent fabric, copper nanoparticles

1. Introduction

Nanotechnology is a rapidly growing field that involves the fabrication and production of nanoparticles with controlled size, shape, and dispersion, with a focus on harnessing their potential for the benefit of humanity. Although physical and chemical methods may yield pure and well-known products (Nadagoudan et al., 2009), metal nanoparticles have found applications in various scientific and industrial domains (Shipway et al., 2000; Rao and Nath, 2003). Silver nanoparticles, in particular, have attracted significant attention due to their excellent conductivity, chemical stability, catalytic properties, as well as photonic and optoelectronic characteristics (Hussain and Pal, 2008). Copper nanoparticles, when reduced to the nanoscale, exhibit entirely different behaviors compared to their bulk counterparts (Habibi et al., 2010).

A variety of chemical methods have been introduced for the synthesis of nanoparticles, including electrochemical methods, physical and ion induction methods (Bréchignac et al., 2008), laser pyrolysis (Rao et al., 2007), microemulsion techniques (Zhang et al., 2007), reduction of metal salts (Yonezawa et al., 2008), two-dimensional crystal methods (Zhang et al., 2007), microwave-assisted synthesis (He et al., 2007), as well as biochemical or green synthesis methods (Kowshik et al., 2002).

One of the main drawbacks of conventional chemical reduction methods is the use of reducing agents that can potentially pose health and environmental hazards, in addition to often being expensive (Aghbali Boroujeni, 2012). Consequently, green synthesis methods for nanoparticles have recently been developed and gained attention in order to produce environmentally friendly and cost-effective nanoparticles. In this study, green synthesis of nanoparticles using polysaccharides is employed as an alternative approach to obtain nanoparticles with desirable properties, such as enhanced water repellency.

In recent years, numerous green synthesis strategies have been reported for the fabrication of metal nanoparticles, many of which rely on plant extracts as natural reducing and stabilizing agents. While these methods are environmentally benign, they often suffer from inherent drawbacks, including compositional variability, low reproducibility, and challenges in scalability—largely due to the complex and inconsistent nature of phytochemical constituents.

In the present study, we introduce an alternative, well-defined, and reproducible green synthesis route by employing low-molecular-weight carbohydrates namely maltose and sucrose as in situ reducing agents for the fabrication of Ag/Cu hybrid nanoparticles. These disaccharides offer a chemically uniform and biocompatible alternative to plant-based systems, enabling precise control over the redox environment and facilitating predictable nanoparticle formation.

Moreover, the use of such carbohydrates is directly compatible with the pad–dry–cure finishing process, eliminating the need for extract preparation or pre-processing steps typically required in plant-based methods. This tailored approach not only enhances consistency and scalability, but also ensures seamless integration into industrial textile functionalization workflows. As such, the

proposed method distinguishes itself from conventional green synthesis techniques and offers a promising pathway toward sustainable, high-performance textile treatments.

2. Materials and Methods

2.1. Materials

A 100% cotton woven fabric with a warp and weft density of 25 per centimeter was procured from Yazdbaf Company. The chemicals used in this study included silver nitrate, copper nitrate, sodium carbonate, maltose, ascorbic acid, and a dispersant, all supplied by Merck, Germany.

For the analysis of the samples, the following instruments were utilized:

- Reflectance spectrophotometer (X-rite Color-Eye 7000A) for reflectance spectra measurements
- Absorption spectrophotometer (Brite model) for determining sample absorbance
- Scanning electron microscope (SEM, Kyky-EM3200 model)
- X-ray powder diffraction (XRD, Equinox 3000 model)
- X-ray microprobe (Horiba Xpma 7200XGT model)
- Tensile tester (Tensometric Rochdale M500-25CT model)
- Martindale abrasion resistance tester (Nasj Sang model)
- Thickness gauge (SDL Atlas, KO94 model)
- Bending stiffness tester (Nasj Sang model)

2.2. Experimental Procedure

The test samples were prepared for the green synthesis of copper/silver hybrid nanoparticles according to Table 1. Ascorbic acid was added to all samples in amounts sufficient to adjust the bath pH to 5, and the samples were impregnated at 50°C for 60 minutes. After completion of the treatment, the samples were dewatered and used for subsequent characterization tests.

Table 1. Sample Coding

Sample code	$A_1/C_1.M_1$	$A_2/C_2.M_1$	$A_1/C_1.M_2$	$A_2/C_2.M_2$
Silver Nitrate Concentration $\%\frac{W}{V}$	0.5	1	0.5	1
Copper Nitrate Concentration $\%\frac{W}{V}$	0.5	1	0.5	1
Maltose Concentration $\%\frac{W}{V}$	1	1	3	3
Dispersant $\%\frac{W}{V}$	2	2	2	2

3. Results

3.1. XRD Analysis

The synthesized nanoparticles were identified using X-ray diffraction (XRD) analysis. XRD patterns were recorded using a Philips X'Pert Pro diffractometer equipped with Cu Kα radiation (λ = 1.5406 Å), operated at 40 kV and 30 mA. The scan was performed over a 2θ range of 10°–130°, with a scan rate of 1°/min and a step size of 0.02°.

The spectra from the samples were obtained using a voltage of 40 kV and a current of 30 mA. Charts 8 and 9 present the XRD patterns of the untreated cotton samples before nanoparticle synthesis and after synthesis, respectively. By analyzing the XRD spectra, one can determine the morphology, composition, and crystal size of the existing particles.

Based on the fiber morphology, the XRD spectra obtained for the three samples were used, together with the Debye–Scherrer equation, to calculate the crystallinity of the synthesized nanoparticles on the fabric. For XRD analysis, powder samples are required; therefore, the fabric samples were converted to powder using a furnace at 600°C for 3 hours. At this temperature, all organic substances are decomposed and eliminated, leaving only the inorganic components.

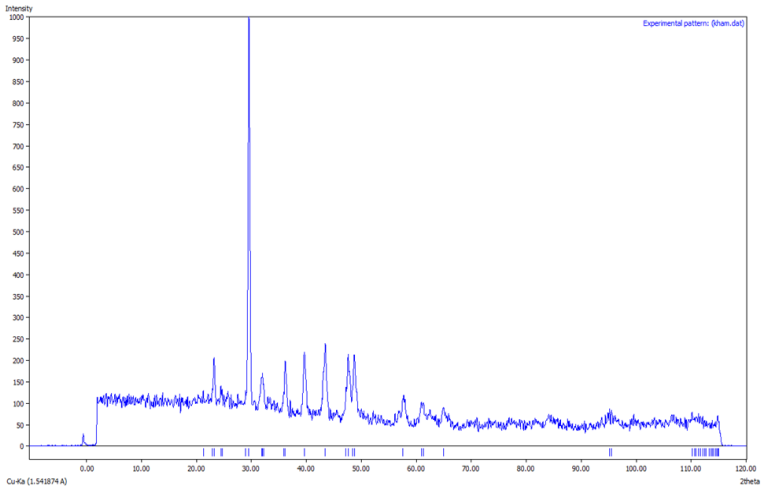

Chart 1. XRD Pattern of the Untreated Cotton Sample

As seen in the XRD pattern of the untreated cotton sample, the peak corresponding to cellulose is observed in the 2θ range of 10–30 degrees. Other peaks may be attributed to impurities present in the cotton fiber, such as fundamental impurities like cobalt and aluminum from agricultural fertilizers, or other factors such as the cotton variety and the presence of dust particles on the fiber.

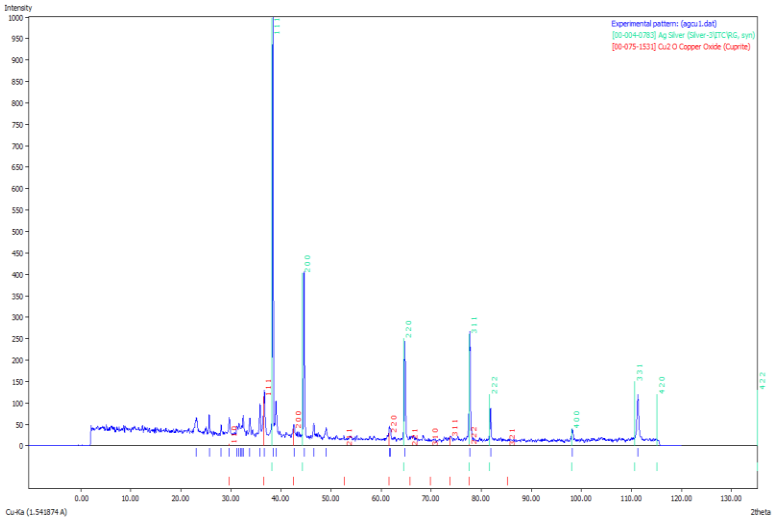

Chart 2. XRD Pattern of Silver/Copper Nanoparticles Synthesized with Maltose as the Reducing Agent (A1/C1.M1)

As observed in the XRD pattern shown in Chart 2, the peak corresponding to silver nanoparticles appears at 2θ ≈ 38°, while the copper peak, which is present as copper oxide due to its reactivity, is observed at approximately 2θ ≈ 43°. To determine the crystallinity of the silver and copper particles, the Debye–Scherrer equation, as described below, can be used.

Scherrer equation $$\tau = \frac{K\lambda}{\beta\cos\theta}$$ 1 Equation

where K is a constant equal to 0.9, λ is the X-ray wavelength (1.54056 Å), β is the FWHM value, τ is the particle size, and θ is the Bragg angle corresponding to the diffraction peak.

Table 2. Degree of Crystallinity

sample		2θ	FWHM	crystallinity
($A_1/C_1.M_1$)	Ag	38.3795	0.1617	9.0798
	Cu	42.5815	0.1881	7.9137

According to Equation1 , the crystallinity values of silver and copper, as well as the FWHM after synthesis, are summarized in Table 2. Based on Table 2, the degree of crystallinity in the ($A_1/C_1.M_1$) sample was determined using the Scherrer equation. According to the standard peaks for silver and copper, the presence of silver and copper nanoparticles in the ($A_1/C_1.M_1$) sample is evident. The data indicate that, due to the high molecular weight and strong reducing power of maltose in the ($A_1/C_1.M_1$) sample, as well as the higher chemical potential of silver compared to copper, the synthesized silver nanoparticles exhibited a higher growth rate than copper nanoparticles under identical conditions.

Although previous reports have described the frequent formation of CuO under aqueous or oxidative conditions—especially at elevated temperatures (Ramasamy, 2013; Thanh, 2014) no characteristic diffraction peaks corresponding to CuO were observed in the treated samples. The elemental analysis (Table 7) indicated the presence of a low amount of CuO (0.15 wt.%), which likely falls below the detection limit of the XRD, particularly if the CuO phase is poorly crystalline or nano-sized. Moreover, the strong diffraction signals of Ag and Cu_2O may have overlapped or masked the weaker reflections of CuO. Additionally, EDX analysis, being elemental in nature, lacks the resolution to distinguish between different copper oxide phases. Thus, the absence of detectable CuO in both XRD and EDX is consistent with instrumental limitations and the low concentration of this phase in the sample.

3.2. Reflectance Evaluation of the Samples

To evaluate the color strength (K/S) of the fabric and measure the color indices (L*a*b*), the yellowness index was determined according to ASTM D1925, and the whiteness index of the samples was measured using the CIE Ganz 82 standard. The reflectance (R) of the samples was measured using a reflectance spectrophotometer, and subsequently, the color strength values (K/S) were calculated using the Kubelka–Munk equation (Equation 1).

Here, R represents the reflectance, K denotes the absorption coefficient, and S is the scattering coefficient.

$$(1) \qquad K/S = \frac{(1-R)^2}{2R} \qquad .$$

Furthermore, the color difference (ΔE) of the samples was calculated using Equation 2. L* indicates the lightness of the samples, a* represents the red-green value, and b* denotes the yellow-blue value of the samples.

$$(2) \qquad \Delta E = \sqrt{\Delta L^{*2} + \Delta a^{*2} + \Delta b^{*2}}$$

The results obtained from the analysis of fabrics containing synthesized nanoparticles, as measured by the reflectance spectrophotometer, are presented in Table 3.

Table 3. Results of the Measured Values for K/S, Yellowness, Whiteness, and ΔE of the Samples

Sample code	L*	a*	b*	K/S	yellowness	whiteness	ΔE
($A_1/C_1.M_1$)	58.177	2.481	9.432	2.358	28.332	-37.257	21.576
($A_2/C_2.M_1$)	57.28	2.62	8.475	2.281	26.585	-32.423	22.429
($A_1/C_1.M_2$)	65.941	1.294	8.889	1.487	23.147	-19.131	13.734
($A_2/C_2.M_2$)	61.629	1.834	8.16	2.067	23.321	-22.603	18.027

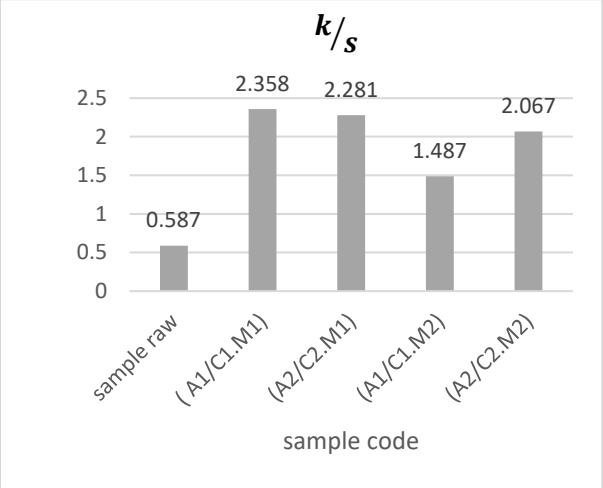

Chart 4. ΔE Values of the Samples

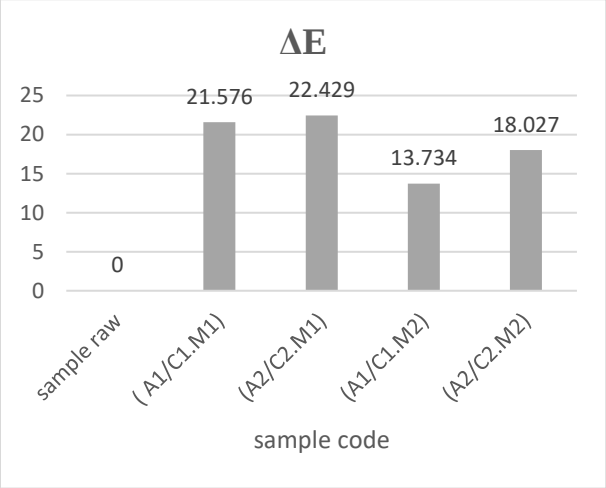

Chart 3. K/S Values of the Samples

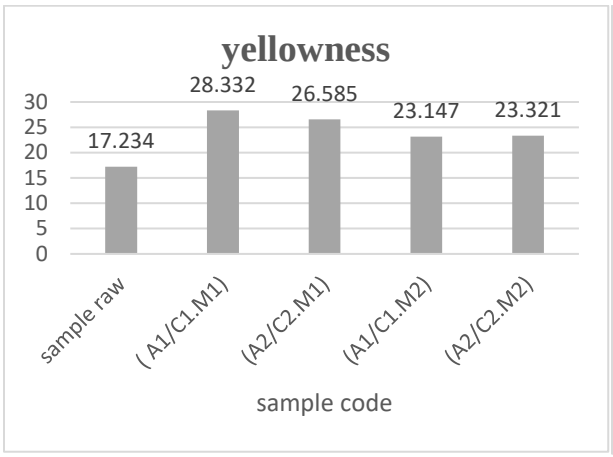

Chart 5. Yellowness Values of the Samples

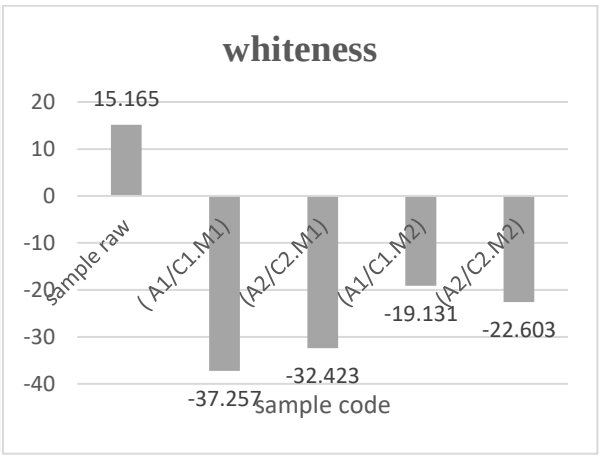

Chart 6. Whiteness Values of the Samples

To investigate the reflectance variations of the samples, an absorption spectrophotometer was used, and the results at the maximum wavelength of 370 nm are presented in Table 3. According to Chart 4, it is evident that this synthesis method allows for an increase in yellowness. Based on Charts 3 to 6, it is clear that sample $A_1/C_1.M_2$ is the optimal sample in this group and is in the best visual condition. This is attributed to the increased number of reducing groups provided by maltose, which enhances the reducing power and thus leads to a higher amount of synthesized silver and copper nanoparticles. Consequently, this results in an increase in whiteness, as well as a decrease in yellowness, K/S, and ΔE values.

3.3. Wicking Test

To evaluate moisture absorption, the wicking test was performed according to AATCC 197-2013 standard.
The data obtained from all samples, along with their comparison to the untreated cotton fabric, are presented in Chart 5 below.

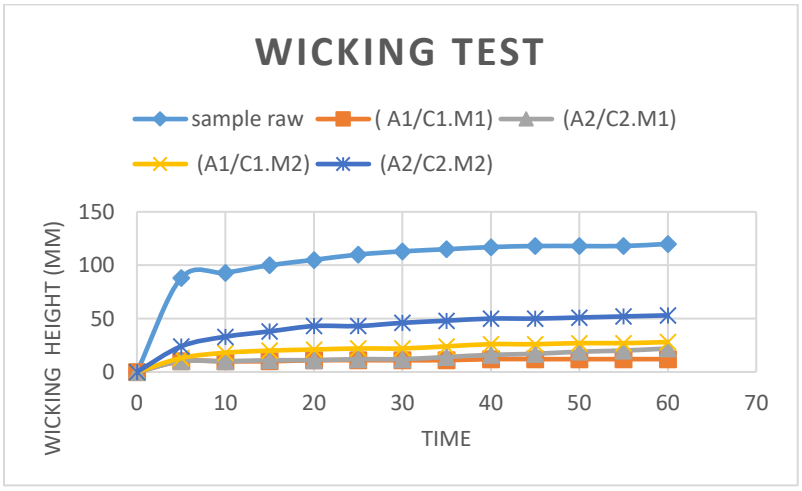

Chart 7. Wicking Test Results of the Samples and Their Comparison with the Untreated Sample

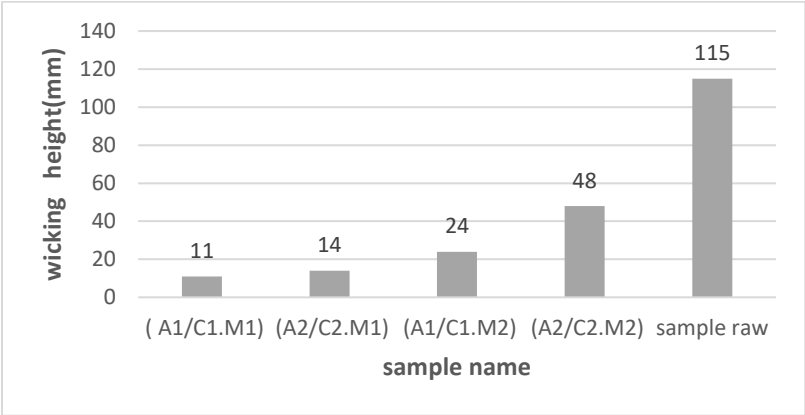

Chart 8. Wicking Results of the Samples at 35 Seconds

In Chart 8, the results at the point of reaching near-equilibrium over 35 minutes are presented. The lower the wicking value in the fiber, the greater the water-repellent property of the fabric. Due to the presence of active groups in the maltose structure, the silver and copper salts, which are ionized in aqueous environments, are reduced and result in the synthesis of nanoparticles of these compounds on the cotton surface. Similar to other metallic salts, these nanoparticles impart water-repellent properties to the fabric, a phenomenon that is clearly reflected in the results shown in Chart 8. reported by Kalyani & Khandelwal (2021), who studied in situ modification of bacterial cellulose with chitosan. Their results demonstrated a decrease in water uptake and retention due to pore volume reduction and densification of the cellulose network. Similarly, in our study, the deposition of Ag/Cu hybrid nanoparticles formed a hydrophobic coating layer on the fabric surface, reducing moisture transport and capillary action. The mechanism of reduced surface porosity and enhanced surface compactness appears to be a common factor contributing to water repellency in both systems (Kalyani & Khandelwal, 2021).

3.4. Drop Test

To assess the rate of moisture absorption, the drop test was performed according to ASTM TS-018 standard. The results, as shown in the table below, indicate that sample ($A_1/C_1.M_1$) exhibits the lowest water absorption.

Table 4. Results of the Drop Test

Sample code	Time (minutes)
Sample raw	0.4
($A_1/C_1.M_1$)	14.50
($A_2/C_2.M_1$)	38.71

($A_1/C_1.M_2$)	12.21
($A_2/C_2.M_2$)	14.08

Figure 1. Images of the Drop Test

3.5. Wash Fastness Evaluation

To assess the wash fastness of the samples, the washing procedure was performed according to ASTM D435-42 (1995) standard. After washing, the water repellency of the fabrics was measured using the drop test. The washing process was conducted once using detergent and sodium carbonate, and the samples were dried at room temperature.

The results indicate that washing reduces the water repellency of the samples; however, even after a single wash, the treated sample retained a significant portion of its water-repellent property compared to the untreated sample.

Table 5. Drop Test Results After One Wash

Sample code	Time(second)
Sample raw	4
($A_1/C_1.M_1$)	80
($A_2/C_2.M_1$)	15.33
($A_1/C_1.M_2$)	4.49

($A_2/C_2.M_2$)	3

3.6. Tensile Strength test

According to ASTM D1445-95, the tensile strength test was performed on all treated samples as well as the untreated control sample. The average percentage of breaking force was determined using the tensile tester software, and the results are presented in Table 6.

Table 6. Percentage of Breaking Force in the Samples

Sample code	٪Force at break
($A_1/C_1.M_1$)	2.81
($A_2/C_2.M_1$)	10.56
($A_1/C_1.M_2$)	-3.52
($A_2/C_2.M_2$)	-6.69

With increasing maltose concentration, the number of acidic ions generated from the decomposition of silver and copper salts increases (according to reactions 1 and 2). This leads to a higher concentration of acidic radicals in the solution, which subsequently results in a reduction in tensile strength. Among the available samples, sample $A_2/C_2.M_1$ exhibits optimal strength.

3.7. SEM Analysis

To examine the surface morphology, particle size, and size distribution, SEM images were obtained from the available samples. The results were analyzed based on the acquired images. Figures 2 to 3 present the SEM images of the untreated cotton sample and the optimized samples ($A_1/C_1.M_1$).

SEM analysis was carried out using a KYKY-EM3200 scanning electron microscope operated at an accelerating voltage of 20 kV. Images were captured at magnifications ranging from 1,000× to 10,000× using 1 μm and 10 μm scale bars to enable both micro- and macro-level surface observations. Prior to imaging, the fabric samples were sputter-coated with a thin gold layer (~10 nm) to improve surface conductivity and prevent charging under the electron beam.

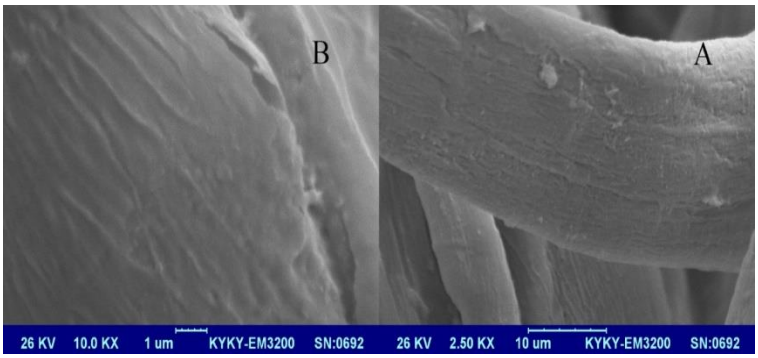

Figure 2. SEM Images of Untreated Cotton Fabric at 2500× Magnification (A) and 10,000× Magnification (B)

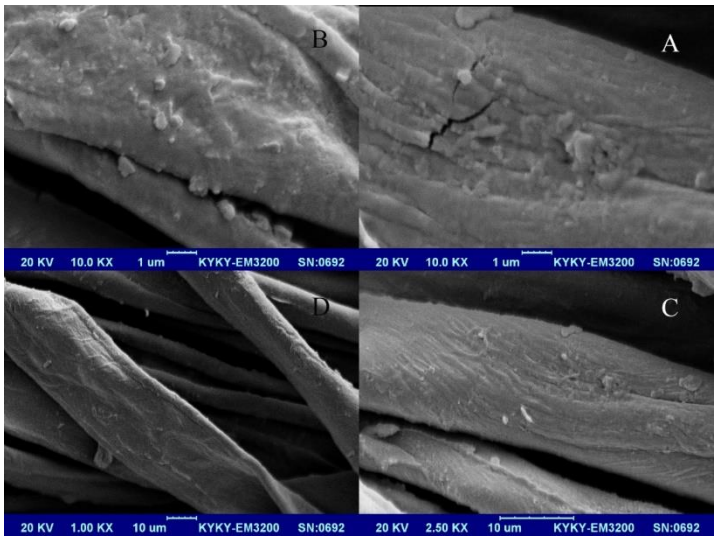

Figure 3. SEM Images of the Optimized Sample ($A_1/C_1.M_1$) at 10,000× Magnification (A, B), 2,500× Magnification (C), and 1,000× Magnification (D)

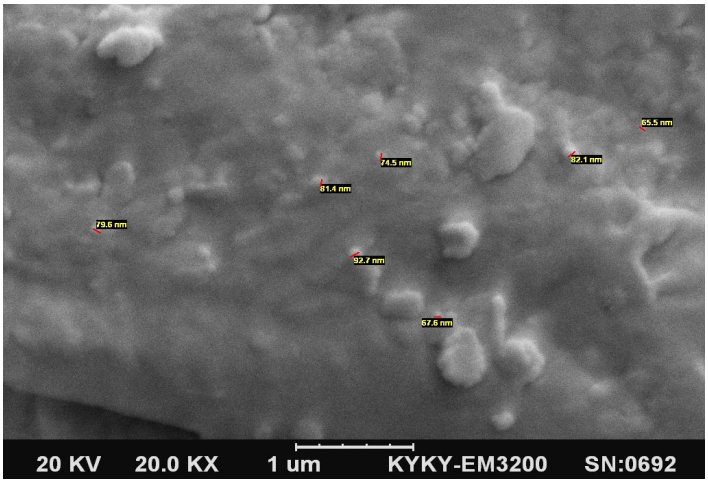

Figure 4. SEM Image of Sample ($A_1/C_1.M_1$) with Indicated Particle Size

As observed in Figures 2 to 3, the fiber surface is completely coated with nanoparticles. These images clearly demonstrate that maltose, due to its high reducing power, has enabled the formation of small and uniform particles in the hybrid sample ($A_1/C_1.M_1$), with the average particle size of this optimized sample being 77.14 nm.

3.8. EDX Analysis

The EDX spectra were obtained from the synthesized samples in order to perform elemental analysis, i.e., to determine the weight and atomic percentages of the constituent elements. Elemental analysis of the optimized samples was conducted using the EDX device in a spot analysis mode, and the results showing the elemental uptake in the fabric are presented in Table 7.

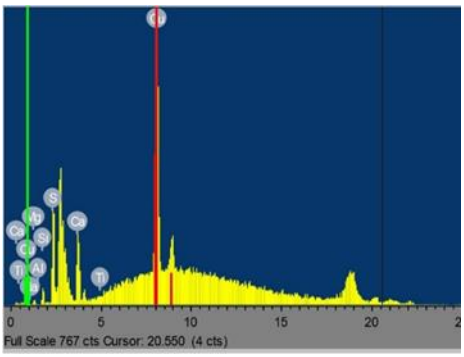

Figure 5. Elemental Analysis (EDX) of Sample ($A_1/C_1.M_1$)

According to Figure 5 and Table 7, the amounts of copper and silver present in the ($A_1/C_1.M_1$) sample are evident. These uptake values were measured at low concentrations, confirming the presence of silver and copper nanoparticles in the sample.

Table 7. Elemental Composition of the Sample ($A_1/C_1.M_1$)

Formula	Mass[%]
Ag_2O	0.01
CuO	0.15

4. Conclusion

In general, the conducted experiments aimed to achieve a cotton fabric with water-repellent properties through the synthesis of copper/silver hybrid nanoparticles. The synthesis of nanoparticles was confirmed by scanning electron microscopy (SEM) and the results of XRD and EDX analyses. The water repellency of the fabric was evaluated using wicking and drop tests. The

tensile strength of the textile was also assessed. Based on the overall results of the tables, charts, and analyses, it was concluded that the fabric exhibits appropriate water repellency, with sample $A_1/C_1.M_1$ demonstrating optimal performance.

References

[1] Santhosh PB, Genova J, Chamati H. Green Synthesis of Gold Nanoparticles: An Eco-Friendly Approach. *Chemistry*,4(2):345-369, 2022.

[2] Lu X, Suslick KS, Li Z. Nanoparticle Optical Sensor Arrays: Gas Sensing and Biomedical Diagnosis. Adv Sensor Res,2(3):22000050, 2022.

[3] Serra M, Arenal R, Tenne R. An overview of the recent advances in inorganic nanotubes. Nanoscale,11(17):9902-9924, 2019.

[4] Arai S. Fabrication of Metal/Carbon Nanotube Composites by Electrochemical Deposition. Electrochem,2(4):563-589, 2021.

[5] Shaheen M, Kalwar NH, Intisar A, Batool Z, Rasheed S, Kousar R. Efficient surfactant modified copper oxide nanoparticles for solar light driven water purification. Optical Materials,122(Pt A):111688, 2021.

[6] Zambon A, Córdoba M. Nanomaterials and Intertheoretical Relations: Macro and Nanochemistry as Emergent Levels. Foundations of Science,26:355-370,2021.

[7] Afreen S, Muthoosamy K, Manickam S. Sono-nano chemistry: A new era of synthesising polyhydroxylated carbon nanomaterials with hydroxyl groups and their industrial aspects. Ultrason Sonochem,51:451-461,2019.

[8] Baig N, Kammakakam I, Falah W. Nanomaterials: a review of synthesis methods, properties, recent progress, and challenges. Mater Adv,2(6):1821-1871,2021.

[9] Losch P, Huang W, Goodman ED, Wrasman CJ, Holm A, Riscoe AR, Schwalbe JA, Cargnello M. Colloidal nanocrystals for heterogeneous catalysis. Nano Today, 24:15-47,2019.

[10] Chhikara BS, Varma RS. Nanochemistry and Nanocatalysis Science: Research advances and future perspectives. J Mater NanoSci,6(1):1-7,2019.

[11] Astruc D. Introduction: Nanoparticles in Catalysis. Chem Rev,120(2):461-463,2020.

[12] Kolahalam LA, Viswanath IVK, Diwakar BS, Govindh B, Reddy V, Murthy YLN. Review on nanomaterials: Synthesis and applications. Mater Today Proc,18(6):2182-2190,2019.

[13] Restrepo CV, Villa CC. Synthesis of silver nanoparticles, influence of capping agents, and dependence on size and shape: A review. Environ Nanotechnol Monit Manag,15:100428,2021.

[14] Ammar HA, Abd El Aty AA, El Awdan SA. Extracellular myco-synthesis of nano-silver using the fermentable yeasts Pichia kudriavzevii HA-NY2 and Saccharomyces uvarum HA-NY3, and their effective biomedical applications. Bioprocess Biosyst Eng,44:841-854,2021.

[15] Yaqoob AA, Umar K, Ibrahim MNM. Silver nanoparticles: various methods of synthesis, size affecting factors and their potential applications—a review. Appl Nanosci. ,10:1369-1378,2020.

[16] Ramasamy, P., & Lee, J. Controlled synthesis of CuO nanostructures and their morphological influence on supercapacitor properties. *Journal of Materials Chemistry A*, 1(4), 1454–1460, 2013.

[17] Thanh, N. T. K., Maclean, N., & Mahiddine, S. Mechanisms of nucleation and growth of nanoparticles in solution. *Chemical Reviews*, 114(15), 7610–7630, 2014.

[18] Kalyani, P., & Khandelwal, M. *Modulation of morphology, water uptake/retention, and rheological properties by in-situ modification of bacterial cellulose with the addition of biopolymers*. Cellulose, 28(17), 1–12, 2021.